# Electron-Electron Interaction in Projectile Ionization Investigated by High Resolution Recoil Ion Momentum Spectroscopy

R. Dörner,[1] V. Mergel,[1] R. Ali,[2] U. Buck,[3] C.L. Cocke,[2] K. Froschauer,[1] O. Jagutzki,[1] S. Lencinas,[1] W.E. Meyerhof,[4] S. Nüttgens,[1] R.E. Olson,[5] H. Schmidt-Böcking,[1] L. Spielberger,[1] K. Tökesi,[6] J. Ullrich,[7] M. Unverzagt,[1] and W. Wu[2]

[1] *Institut für Kernphysik, Universität Frankfurt, D60486 Frankfurt, Germany*
[2] *Department of Physics, Kansas State University, Manhattan, Kansas 66506*
[3] *MPI für Strömungsforschung, W-3400 Göttingen, Germany*
[4] *Department of Physics, Stanford University, Stanford, California 94305*
[5] *Department of Physics, University of Missouri-Rolla, Rolla, Missouri 65401*
[6] *ATOMKI, H4001 Debrecen, Hungary*
[7] *Gesellschaft für Schwerionenforschung Darmstadt mbH, D6100 Darmstadt, Germany*

(Received 22 December 1993; revised manuscript received 7 April 1994)

Contributions of the electron-electron and the nuclear-electron interactions to projectile electron loss in $He^+$ on helium collisions have been clearly separated kinematically for the first time by measuring the longitudinal and transverse momenta of the recoiling target ion with precision of better than $\pm 0.15$ a.u. The longitudinal and transverse momentum distributions are in general agreement with two-center $n$-body classical trajectory Monte Carlo calculations.

PACS numbers: 34.50.Fa, 34.70.+e

In fast ion-atom collisions, a projectile can be ionized due to the Coulomb interaction of the active projectile electron with the target nucleus ($n$-$e$) or with one of the target electrons ($e$-$e$) [1]. In Ref. [2] an experimental separation of these processes for the limit of high impact energies was demonstrated by means of coincident target and projectile charge-state total cross section measurements. Prior attempts to separate these processes had to rely mainly on theory [3–7], although in [8] a separation of the $e$-$e$ process was effected for the first time in a spin-flip transition and in [9] scattering angle dependent measurements were made which partly effected a separation.

In this work we present measurements of the recoil ion momentum transverse and longitudinal to the beam direction ($p_{\perp_{rec}}$ and $p_{\|_{rec}}$) for the reactions

$$He^+ + He \rightarrow He^{2+} + He^+ + 2e^-, \quad (1)$$

$$e^- + He \rightarrow He^+ + 2e^- \quad (2)$$

for impact energies between 0.5 and 2 MeV for (1) and 130 eV impact energy for (2). These doubly differential cross sections $d^2\sigma/dp_{\perp_{rec}}\,dp_{\|_{rec}}$ illuminate in great detail the characteristic momentum exchange patterns of the different interaction processes. This allows for all impact energies a clear experimental separation of the $e$-$e$ process from processes where the target nucleus is actively involved. The comparison between the differential cross section for reactions (1) and (2) demonstrates in addition the similarities for target ionization by bound and by free electron impact. Two types of $n$-$e$ processes can contribute to reaction (1). The projectile electron can be emitted to the continuum $n$-$e_{ion}$ combined with a simultaneous single ionization of the target, or it can be captured into the target potential $n$-$e_{capt}$ if this is accompanied by a double ionization of the target.

While the $n$-$e_{ion,capt}$ process can occur at all projectile velocities, the $e$-$e$ process has a threshold due to the fact that the target electron, as seen from the projectile frame, must have sufficient energy that it can ionize the projectile and simultaneously escape from the target. For $He^+$ on He, this threshold is near 0.4 MeV [2]. In addition to the different impact energy dependence of the $e$-$e$ and $n$-$e_{ion,capt}$ contributions, one can expect the momentum exchange between the collision partners to be very different for the two mechanisms. For the $e$-$e$ interaction, the target nucleus mainly acts as a spectator to the process. Therefore, very little momentum will be transferred between projectile electron and the target nucleus. In the case of the $n$-$e_{ion,capt}$ interaction the target nucleus has to exchange enough momentum with the projectile electron to either capture it or eject it into the continuum. This will result in differences in the longitudinal recoil ion momentum distribution. Furthermore, the main contribution of the $e$-$e$ interaction can be expected at larger impact parameters, i.e., smaller transverse momentum transfer, between the two nuclei, than the contribution of the $n$-$e_{ion,capt}$ interaction [10].

The momentum transfer in the reaction under study lies in the range of a few a.u. and the difference between the $e$-$e$ and $n$-$e_{ion,capt}$ contribution is $< 1$ a.u. For this measurement, we have developed a recoil ion momentum spectrometer [11] based on a cooled supersonic gas jet. So far a resolution of about 1.6 a.u. for $p_{\perp_{rec}}$ (equivalent to a recoil ion energy of 5 meV for helium) [11–13] had been reported and of about 4 a.u. for a measurement of $p_{\|_{rec}}$ [14,15] only. Our novel technique allows, for the first time, a measurement of $p_{\perp_{rec}}$ and $p_{\|_{rec}}$ with a resolution of about $\pm 0.15$ a.u., equivalent to a recoil ion energy of



0031-9007/94/72(20)/3166(4)$06.00

© 1994 The American Physical Society

$\pm 40$ $\mu$eV.

A $He^+$ beam from the Van de Graff accelerator at the Institut für Kernphysik in Frankfurt is collimated to a beam spot of about 0.2 mm×0.2 mm. The ion beam intersects with a cold supersonic He gas jet. The projectiles are charge state analyzed by electrostatic deflectors before and after the collision region and detected by a position sensitive channel plate detector. The data for electron impact have been obtained using a pulsed electron gun. The recoil ions created at the intersection point are extracted by a homogeneous electric field of 0.33 V/cm perpendicular to both the ion beam and the He gas jet. After traversing 3 cm in this field the ions enter a field free drift region of 6 cm length and are then postaccelerated by 2300 V over 2 mm onto a position sensitive channelplate detector of 4 cm diameter and a position resolution of below 0.2 mm FWHM.

The cold localized He target is created using a cooled supersonic expansion through a 30 $\mu$m hole. The gas source with the hole is mounted on the cold finger of a cryopump and cooled to 20 K. At a distance of about 1 cm the expanding gas is collimated by a skimmer of 0.3 mm diameter. The gas jet at the collision point about 3 cm away from the skimmer has a diameter of 1.1 mm and the local gas density is $5 \times 10^{11}$ atoms/cm$^2$.

From the time of flight of the recoil ions, the momentum component in the field direction and the charge state are obtained. The two momentum components perpendicular to the extraction are calculated from the position of the ion on the recoil channel plate and the time of flight. In a separate experiment using a capture reaction the momentum resolution was measured to be below $\pm 0.15$ a.u. The $p_{\|_{\rm rec}} = 0$ point was determined with a precision of $\pm 0.05$ a.u. by measuring $p_{\|_{\rm rec}}$ for single electron capture by $He^+$ and $He^{2+}$ ions at various impact energies [13]. A more detailed discussion of the experimental setup will be given in a forthcoming paper.

In Fig. 1 the experimental double differential cross sections $d^2\sigma/dp_{\perp_{\rm rec}}dp_{\|_{\rm rec}}$ are shown for reaction 1 for different projectile energies (a)–(e) together with the data for electron impact (f). At 1 MeV impact energy two maxima in the experimental double differential cross section can clearly be observed. The momentum distribution of the $He^+$ ions created by equal velocity electron impact [Fig. 1(f)] demonstrate that the contribution with the maximum at small momenta is due to the $e$-$e$ interaction. We will show below that the second maximum can be attributed to the $n$-$e_{\rm ion,capt}$ mechanism. With increasing energy the contribution at higher momenta disappears while for lower impact energies the maximum at small momentum transfers vanishes.

The contribution of the $e$-$e$ interaction should show an approximate threshold near a projectile energy of 0.4 MeV, equivalent to an electron energy of 54 eV, the projectile binding energy. To achieve simultaneous target and projectile ionization only one Coulomb interaction is necessary for the $e$-$e$ process . In the case of the $n$-$e_{\rm ion}$ process two Coulomb interactions (projectile nucleus with one of the target electrons and target nucleus with the projectile electron) and for the $n$-$e_{\rm capt}$ process three interactions are needed (the projectile ionizing both target electrons plus a capture of the projectile electron by the target nucleus). Therefore in the limit of high energies the cross section for the $e$-$e$ process can be expected to scale like $1/(E \ln E)$ and like $1/(E^2 \ln E)$ for the $n$-$e_{\rm ion}$ process. Since velocity matching is required for the

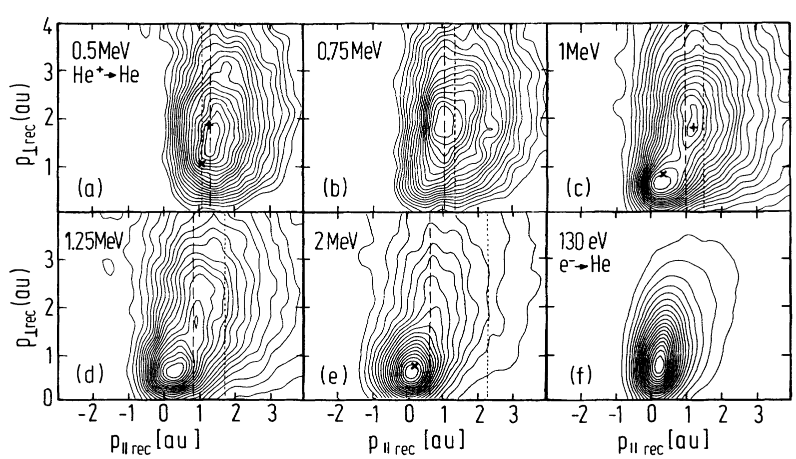


FIG. 1. Doubly differential cross sections for the reactions (1) and (2). The $y$ axis shows the momentum of the recoiling $He^+$ ions perpendicular to the beam axis; the $x$ axis the momentum in beam direction (positive value means forward emission). The contour lines are linear and equally spaced in cross section. The long dashed line marks the estimated $p_{\|_{\rm rec}}$ peak position of the $n$-$e_{\rm ion}$ process and the short dashed line of the $n$-$e_{\rm capt}$ process (see text). The × and the + mark the maxima of the nCTMC cross section for the $n$-$e_{\rm ion}$ + $e$-$e$ and $n$-$e_{\rm capt}$ processes, respectively. (f) The same data for 130 eV electron impact, which is comparable in velocity to 1 MeV $He^+$.

$n$-$e_{\rm capt}$ process, it will decrease even faster with increasing projectile energy and will only contribute at the low impact energies. The $n$-$e_{\rm ion}$ process can be expected to dominate in an intermediate energy range. The $e$-$e$ interaction will dominate the cross section for simultaneous projectile and target ionization in the high energy limit [2].

We now estimate the most probable target recoil momenta for the different processes. If the projectile is ionized the binding energy ($E_{\rm bind}$) plus the continuum energy ($E_e$) of the emitted electron (seen from the projectile rest frame) is needed. Since there is no other source of energy in the laboratory system, this is taken from the kinetic energy of the projectile. For fast heavy projectiles (i.e., if the energy loss is small compared to the total kinetic energy) this corresponds to a change in longitudinal projectile momentum of [13]

$$\Delta p_{\parallel} = -(E_{\rm bind} + E_e)/v_{\rm pro}. \quad (3)$$

This momentum change of the projectile has to be balanced by the collision partner, either the electron or the target nucleus. For the case of the $e$-$e$ interaction the target electron will therefore be emitted in the forward direction while the target nucleus is a spectator to the process, gaining only very little longitudinal momentum $p_{\parallel_{\rm rec}}$. In the case of the $n$-$e_{\rm ion}$ process, this momentum is gained by the recoil ion. If one further takes the ionized target electron into account, this forward momentum will be enhanced due to the additional binding energy of this target electron and be smeared out and maybe shifted a little due to its continuum momentum distribution. If the projectile and target electrons are emitted into zero energy continuum states with respect to their parent rest frames, one obtains a longitudinal recoil ion momentum of $p_{\parallel_{\rm rec}} = (79\ {\rm eV})/v_{\rm pro}$. This is indicated by the long dashed lines in Fig. 1.

For the case of the $n$-$e_{\rm capt}$ process, one obtains, neglecting the target electrons, a forward momentum of $p_{\parallel_{\rm rec}} = v_{\rm pro}/2$, since the kinetic energy of the captured electron seen from the projectile is given by $E_e = v_{\rm pro}^2/2$ and there is no net change in binding energy for a ground state capture. This value is indicated by the short dashed lines in Fig. 1.

The transverse momentum of the recoil ion is given by the sum of the transverse momenta of all ionized electrons plus the momentum due to the repulsion between the nuclei. It therefore reflects also the information on the impact parameter. Montenegro and Meyerhof first pointed out that the cross section of the $n$-$e_{\rm ion}$ process will be dominated by impact parameters around the shell radius of the projectile while the $e$-$e$ interaction will have their main contributions at larger distances [10]. The data presented here confirm this prediction. The $n$-$e_{\rm capt}$ mechanism also requires close impact parameters since a double ionization is involved.

A comparison of the single differential cross sections with two-center $n$-body classical trajectory Monte Carlo (nCTMC) calculations [16] is made. Briefly, the nCTMC calculations employ all three electrons in reaction (1) and iteratively solve the Hamiltonian

$$H = \frac{p_a^2}{2m_a} + \frac{p_b^2}{2m_b} + \sum_{k=1}^{3} \frac{p_k^2}{2m_e} - \frac{2}{r_{ai}} - \sum_{j=1}^{2} \frac{Z_j^{\rm eff}}{r_{bj}} + \frac{4}{r_{ab}} - \frac{2}{r_{bi}} - \sum_{j=1}^{2} \frac{2}{r_{aj}} + \sum_{j=1}^{2} \frac{1}{r_{ij}}. \quad (4)$$

In Eq. (4), the indices $a$ and $b$ denote the projectile and target nuclei, respectively, while the indices $i$ and $j$ refer to electrons originally on the projectile and target, respectively ($Z_{j=1}^{\rm eff}$=1.6875 and $Z_{j=2}^{\rm eff}$ =2.00). Thus the two-center $e$-$e$ interaction is included with the $n$-$e_{\rm ion}$ in this calculation. Moreover, the $n$-$e_{\rm capt}$ reaction—double ionization of the target concurrent with electron capture from projectile to target—is also included. The calculated total cross section is in good agreement with experimental observation [2, 17]. The results are shown in Fig. 2. At 0.5 MeV impact energy the calculation shows a 37% contribution of the $n$-$e_{\rm capt}$ process, rapidly decreasing with increasing impact energy. The calculated peak positions are shown by the crosses in Fig. 1. The exper-

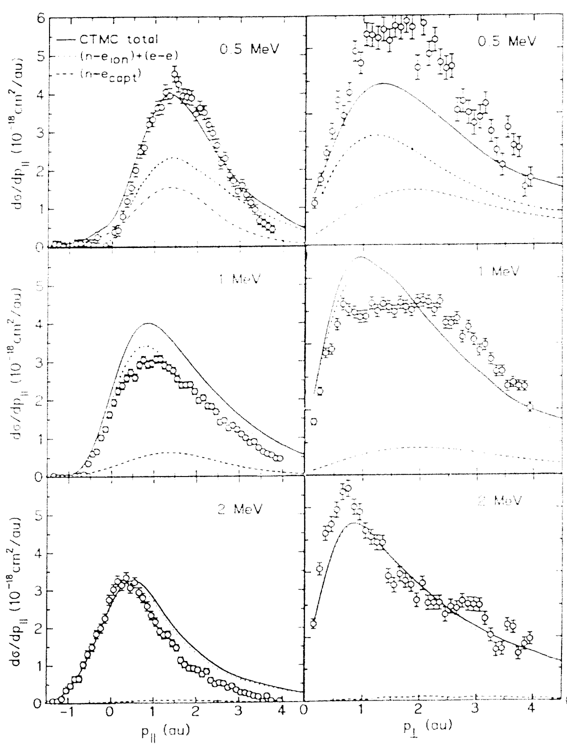


FIG. 2. Single differential cross section for reaction (1). Left column: momentum of the recoil ion longitudinal to the beam axis; right column: momentum perpendicular to the beam axis. Dashed line: two-center nCTMC calculation for the $n$-$e_{\rm capt}$ process; dotted line: $n$-$e_{\rm ion}$ + $e$-$e$ processes; full line: sum of all three processes.

imental data are normalized to total cross sections from [2, 17] to obtain a direct comparison with the calculations. Since our spectrometer does not detect momenta higher than 4 a.u., the absolute values have an uncertainty of ±30%.

In conclusion, we have separated experimentally the contribution of $e$-$e$ interaction to the simultaneous projectile and target ionization, exploiting high resolution recoil ion momentum spectroscopy. Our technique can be used without any restrictions concerning momentum resolution up to relativistic projectile velocities and for all projectile charges. We have demonstrated that the present resolution enables a determination of the $Q$ value of atomic reactions by measuring the recoil ion longitudinal momentum transfer. This may be used to investigate in great detail other reactions such as kinematic, resonant, or radiative electron capture. The technique is ideally suited for differential studies of atomic collision processes in storage rings; such experiments are in preparation.

We are thankful for very helpful discussions with and for calculations by E.C. Montenegro, W. Fritsch, and S. Manson. The work was financially supported by DFG, BMFT, and DOE Grant No. 82ER53128. One of us (W.E.M.) was supported by NSF Grants No. INT-9013087 and No. PHY-9019293. R.A., W.W., and C.L.C. acknowledge financial support from Max Planck Forschungspreis of the Humboldt Foundation.

[1] D.R. Bates and G. Griffing, Proc. Phys. Soc. London A **66**, 961 (1953); **67**, 663 (1954); **68**, 90 (1955).
[2] E.C. Montenegro, W.S. Melo, W.E. Meyerhof, and A.G. dePinho, Phys. Rev. Lett. **69**, 3033 (1992).
[3] J.H. McGuire, N. Stolterfoht, and P.R. Simony, Phys. Rev. A **24**, 97 (1981).
[4] R. Hippler, S. Datz, P.D. Miller, P.L. Pepmiller, and P.F. Dittner, Phys. Rev. A **35**, 585 (1987).
[5] T.N. Tipping, J.M. Sanders, J. Hall, J.L. Shinpaugh, D.H. Lee, J.H. McGuire, and P. Richard, Phys. Rev. A **37**, 2906 (1988).
[6] H.-P. Hülskötter, B. Feinberg, W.E. Meyerhof, A. Belkacem, J.R. Alonso, L. Blumenfeld, E.A. Dillard, H. Gould, G.F. Krebs, M.A. McMahan, M.E. Rhoades-Brown, B.S. Rude, J. Schweppe, D.W. Spooner, K. Street, P. Thieberger, and H.E. Wegner, Phys. Rev. **44**, 1712 (1991).
[7] D.H. Lee, T.J.M. Zouros, J.M. Sanders, P. Richard, J.M. Anthony, Y.D. Wang, and J.H. McGuire, Phys. Rev. A **46**, 1374 (1992).
[8] T.J.M. Zouros, D.H. Lee, and P. Richard, Phys. Rev. Lett. **62**, 2261 (1989).
[9] E.C. Montenegro, A. Belkacem, D.W. Spooner, W.E. Meyerhof, and M.B. Shah, Phys. Rev. A **47**, 1045 (1993).
[10] E.C. Montenegro and W.E. Meyerhof, Phys. Rev. A **46**, 5506 (1992).
[11] J. Ullrich, R. Dörner, S. Lencinas, O. Jagutzki, H. Schmidt-Böcking, and U. Buck, Nucl. Instrum. Methods Phys. Res., Sect. B **61**, 415 (1991).
[12] R. Dörner, J. Ullrich, H. Schmidt-Böcking, and R.E. Olson, Phys. Rev. Lett. **63**, 147 (1989).
[13] R. Dörner, J. Ullrich, O. Jagutzki, S. Lencinas, A. Gensmantel, and H. Schmidt-Böcking, in *Electronic and Atomic Collisions*, Proceedings of the ICPEAC XVII, edited by W. R. MacGillivray, I. E. McCarthy, and M. C. Standage (Adam Hilger, Bristol, 1991), p. 351.
[14] R. Ali, V. Frohne, C.L. Cocke, M. Stöckli, S. Cheng, and M.L.A. Raphaelian, Phys. Rev. Lett. **69**, 2491 (1992).
[15] V. Frohne, S. Cheng, R. Ali, M. Raphaelian, C.L. Cocke, and R.E. Olson, Phys. Rev. Lett. **71**, 696 (1993).
[16] R.E. Olson, *Electronic and Atomic Collisions* (Elsevier Science Publishers, New York, 1988), p. 271.
[17] R.D. DuBois, Phys. Rev. A **39**, 4440 (1989).